

Torque magnetometry studies of new low temperature metamagnetic states in $\text{ErNi}_2\text{B}_2\text{C}$

D. G. Naugle,^{1,*} B. I. Belevtsev,^{2,†} K. D. D. Rathnayaka,¹ S.-I. Lee,³ and S. M. Yeo³

¹*Department of Physics, Texas A&M University, College Station, TX 77843, USA*

²*B. Verkin Institute for Low Temperature Physics and Engineering,
National Academy of Sciences, pr. Lenina 47, Kharkov 61103, Ukraine*

³*National Creative Research Center for Superconductivity and Department of Physics,
Pohang University of Science and Technology, Pohang 790-784, Republic of Korea*

The metamagnetic transitions in single-crystal $\text{ErNi}_2\text{B}_2\text{C}$ have been studied at 1.9 K with a Quantum Design torque magnetometer. The critical fields of the transitions depend crucially on the angle between applied field and the easy axis [100]. Torque measurements have been made while changing angular direction of the magnetic field (parallel to basal tetragonal ab -planes) in a wide angular range (more than two quadrants). Sequences of metamagnetic transitions with increasing field are found to be different for the magnetic field along (or close enough to) the easy [100] axis from that near the hard [110] axis. The study have revealed new metamagnetic states in $\text{ErNi}_2\text{B}_2\text{C}$ which were not apparent in previous longitudinal-magnetization and neutron studies.

The rare-earth nickel borocarbides $\text{RNi}_2\text{B}_2\text{C}$ (where R is a rare-earth element) show unique superconducting and/or magnetic properties. In this report, a torque magnetometry study of metamagnetic transitions at low temperature ($T \approx 1.9$ K) in single-crystal $\text{ErNi}_2\text{B}_2\text{C}$ is presented. Magnetic states in this highly anisotropic compound are determined by magnetic moments of Er ions which lay in the ab -planes^{1,2} along the easy axis in the [100] direction. For tetragonal symmetry inherent in the borocarbides, the [010] direction is an easy axis as well, so that actually four easy axes are available. The hard axes in-plane are situated between equivalent easy axes (for example, in the [110] direction). The crystal lattice of $\text{ErNi}_2\text{B}_2\text{C}$ is characterized by orthorhombic distortion below 2 K, which, however, does not have much influence on angular symmetry of metamagnetic transtions.

In $\text{ErNi}_2\text{B}_2\text{C}$, superconductivity and antiferromagnetism coexists ($T_c \approx 11$ K and $T_N \approx 6$ K). Below T_N the magnetic phases are spin-density wave (SDW) states with the modulation vector $\mathbf{Q} = f\mathbf{a}^*$ (or \mathbf{b}^* , where \mathbf{a}^* and \mathbf{b}^* are reciprocal lattice vectors)^{2,3,4}. For the AFM state at zero field $f \approx 0.55$. Ordered moments are perpendicular to \mathbf{Q} . The SDW phase becomes squared-up below 3 K^{1,2}. Below $T_{WF} \approx 2.5$ K a transition to a weak-ferromagnetic (WF) state occurs, in which a ferromagnetic moment (about $0.33 \mu_B$ per Er ion) appears⁵.

With increasing field (applied in the ab plane) several metamagnetic transitions occur in this compound. The fields of the transitions depend strongly on the angle θ between H and a nearest easy axis (or on the angle ϕ between H and a nearest hard axis)⁶. Generally, the ferromagnetic component increases at each transition reaching the maximum value (about $8 \mu_B/\text{Er}$) at the final transition to the saturated paramagnetic state at $H \gtrsim 2$ T. The metamagnetic states (except the final paramagnetic state) remain SDW, only the scalar f of the wave vector $\mathbf{Q} = f\mathbf{a}^*$ changes slightly, but quite distinctly, at these transitions^{3,4}. The known longitudinal magnetization^{6,7} and neutron diffraction^{3,4} studies of metamagnetic tran-

sitions in $\text{ErNi}_2\text{B}_2\text{C}$ gave rather different results. The magnetization studies^{6,7} at $T = 2$ K revealed four metamagnetic transitions for an easy direction (at fields about 0.7 T, 1.1 T, 1.25 T and 2.0 T) and three transitions for a hard direction (at fields about 1.0 T, 1.4 T and 1.8 T). Also, in the field range above 2.5 T for field directions not far away from a hard axis, a weak feature in field dependence of magnetization was found⁶ which was interpreted as a final transition to the paramagnetic state with a critical field that diverges as $\phi \rightarrow 0$.

Results of the neutron^{3,4} and magnetization^{6,7} studies at $T = 2$ K are mutually consistent only for the first two metamagnetic transitions. Detailed neutron studies⁴ give a rather complex picture of metamagnetic states. In the easy direction, five metamagnetic transitions (with considerable changes in magnetic structure) were found, but only four SDW magnetic structures were distinguished. For the hard direction, three SDW phases were seen, but for a considerable field range the metamagnetic states are mixed-phase states. For both directions a two-domain magnetic state was found with modulation vectors in the domains being perpendicular to each other.

In this study, a PPMS Model 550 Torque Magnetometer is used to study angular dependence of the metamagnetic transitions. It measures the torque $\vec{\tau} = \mathbf{M} \times \mathbf{H}$, so that $\tau = MH \sin(\beta)$, where β is the angle between the external magnetic field and the magnetization. A small (about 0.08 mg) single-crystal rectangular plate of $\text{ErNi}_2\text{B}_2\text{C}$ was used. The torque was measured as a function of magnetic field for different constant angles, or varying angular direction of the field for different constant magnetic fields.

The metamagnetic transitions manifest themselves as sharp changes in field dependences $\tau(H)/H$ at critical fields as shown in Figs. 1 and 2. The angular phase diagram for $\text{ErNi}_2\text{B}_2\text{C}$ obtained is shown in Figs. 3 and 4. The critical fields were defined as the fields of the inflection point of the $\tau(H)/H$ curves, recorded for increasing field. These points were found using derivatives.

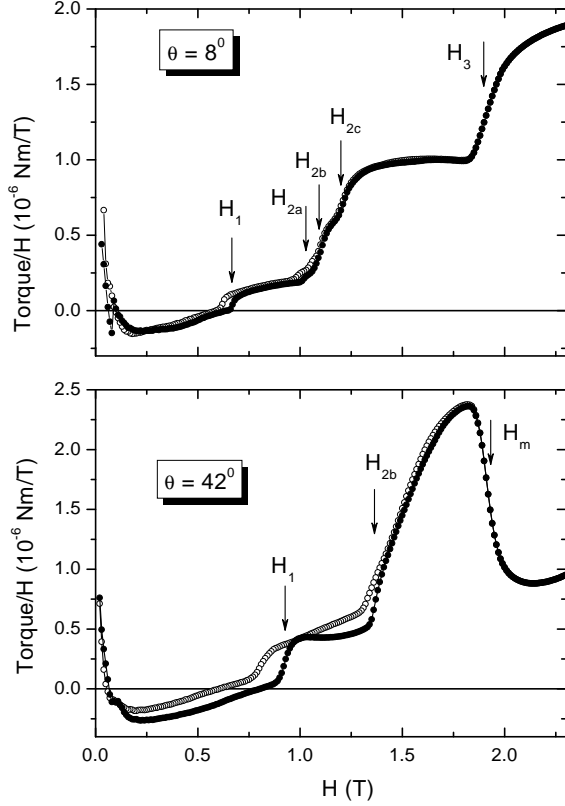


FIG. 1: Dependences $\tau(H)/H$ for increasing and decreasing magnetic field (filled and empty circles, respectively) for field directions close to ($\theta \approx 8^\circ$) and far from ($\theta \approx 42^\circ$) an easy axis. Positions of the transition fields are shown by arrows.

Some points in the phase diagram were determined from torque angular dependences recorded for different fixed fields (Fig. 4).

We have found that the sequence of transitions depends crucially on the angular position of the magnetic field. In the range $-30^\circ \lesssim \theta \lesssim 30^\circ$, with increasing field transitions at critical fields, denoted as H_1 , H_{2a} , H_{2b} , H_{2c} and H_3 take place (see $\tau(H)/H$ curve for $\theta \approx 8^\circ$ in Fig. 1 and angular diagram in Figs. 3 and 4). In the adjoining angular region, $-15^\circ \lesssim \phi \lesssim 15^\circ$, the sequence of transitions includes critical fields H_1 , H_{2b} , H_m and H_{3f} (Figs. 1-4). At fields H_3 and H_{3f} transitions to the saturated paramagnetic state take place. The notation for metamagnetic phases is clear from Figs. 3 and 4. Phases F_{WF} and F_{PM} are the initial WF and the final saturated paramagnetic states, respectively.

In this study, new metamagnetic states have been found. In the range $1.0 \text{ T} \leq H \leq 1.4 \text{ T}$ three closely-spaced transitions (at $H = H_{2a}$, H_{2b} and H_{2c}) for $|\theta| \lesssim 30^\circ$ and only one (at $H = H_{2b}$) for $30^\circ \lesssim |\theta| \lesssim 45^\circ$ ($|\phi| \lesssim 15^\circ$) were seen (Figs. 1-4). These critical fields are proportional to $1/\cos(\theta)$ with $H_{2a}(\theta = 0) \approx 1.02 \text{ T}$, $H_{2b}(\theta = 0) \approx 1.13 \text{ T}$ and $H_{2c}(\theta = 0) \approx 1.27 \text{ T}$. In a previous longitudinal magnetization study only two transitions (at fields which correspond to H_{2b} and H_{2c}) were

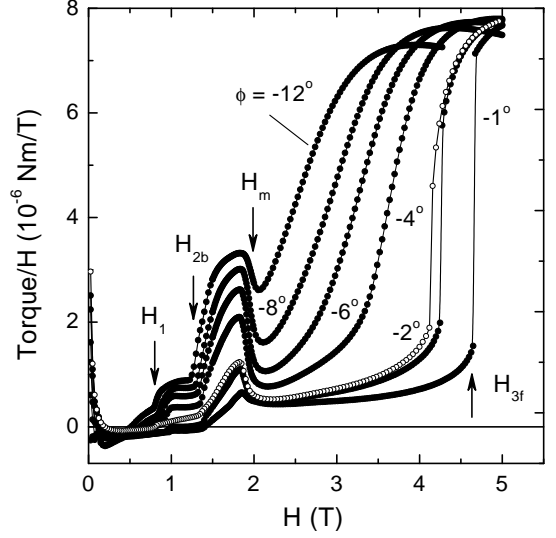


FIG. 2: $\tau(H)/H$ dependences (increasing field) for different angles ϕ relative to the closest hard axis $\langle 110 \rangle$. Positions of the critical fields H_1 , H_{2b} , H_m and H_{3f} are shown by arrows for some of the curves. For $\phi = -2^\circ$, the curves for increasing and decreasing (empty circles) field are shown. A dramatic increase in H_{3f} when field direction goes to $|\phi| = 0$ is evident.

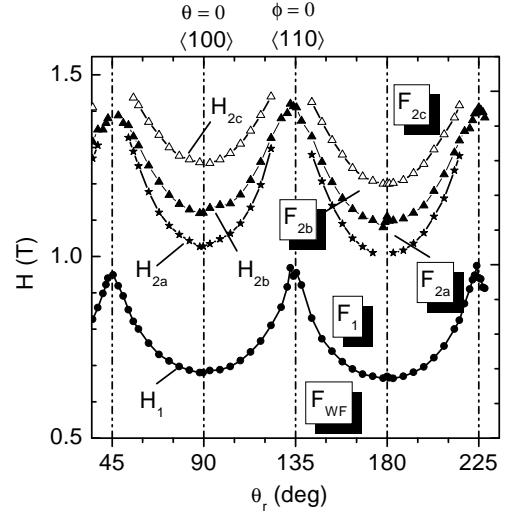


FIG. 3: Low-field part of the angular phase diagram of metamagnetic states in $\text{ErNi}_2\text{B}_2\text{C}$ at $T = 1.9 \text{ K}$. θ_r is angular position of the sample rotator. The positions of easy, $\langle 100 \rangle$, and hard, $\langle 110 \rangle$, axes in one of the quadrants are shown. The H_1 , H_{2a} , H_{2b} and H_{2c} are critical fields of metamagnetic transitions. The symbols F_{WF} , F_1 , F_{2a} , F_{2b} , F_{2c} show regions of existence for different phases.

found in an easy direction at $T = 2 \text{ K}$ within this field range and one (at H_{2b}) for the field in a hard direction⁷. Only one (that at $H = 1.15 \text{ T}$) of the magnetostructural transitions (at $T = 1.8 \text{ K}$ in an easy direction above $H = 1 \text{ T}$) found in the neutron study⁴ corresponds to results of the longitudinal magnetization^{5,7} and this torque

study. The rather weak (but quite clear) transition at H_{2a} , found in this study, was not revealed previously in any study. The high precision and sensitivity of the torque measurements to the normal component of M permit its observation.

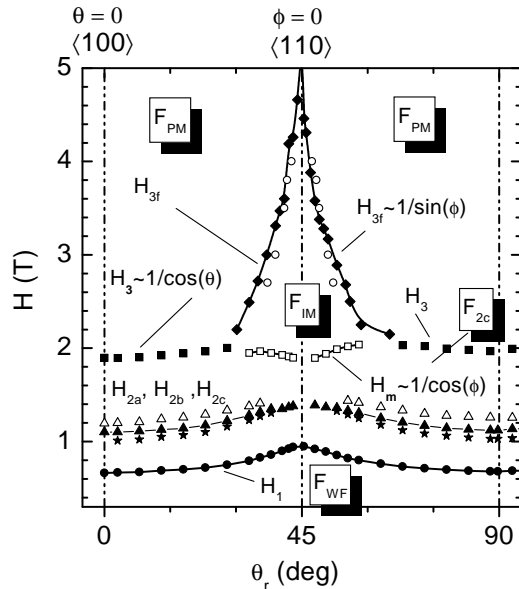


FIG. 4: Angular phase diagram of metamagnetic states in $\text{ErNi}_2\text{B}_2\text{C}$ at $T = 1.9$ K for the field range studied. The angle θ_r is the angle on the sample rotator. The positions of easy, $\langle 100 \rangle$, and hard, $\langle 110 \rangle$, axes are shown. The symbols F_{WF} , F_{2c} , F_{IM} , and F_{PM} show regions of existence for different phases. All data were obtained from $\tau(H)$ curves for different fixed angles except for the open circles which were, obtained from torque angular dependences.

New results were found for fields above 2 T (Fig. 4): a final transition to the saturated paramagnetic state proceeds either directly from phase F_{2c} ($F_{2c} \rightarrow F_{PM}$) for $|\theta| \lesssim 30^\circ$ or through an intermediate phase F_{IM} ($F_{2c} \rightarrow F_{IM} \rightarrow F_{PM}$) for field directions close enough to a hard axis ($30^\circ \lesssim |\theta| \lesssim 45^\circ$). The critical field H_3 for the direct transition ($F_{2c} \rightarrow F_{PM}$) follows approximately the angular relation $H_3(\theta) = H_3(0)/\cos(\theta)$ with $H_3(0) \approx 1.93$ T (for $|\theta| \lesssim 10^\circ$). Transition to the intermediate state ($F_{2c} \rightarrow F_{IM}$) takes place at H_m which is approximately described by $H_m(\phi) = H_m(0)/\cos(\phi)$ with $H_m(0) \approx 1.92$ T. The critical field H_{3f} for transition to the paramagnetic state from the intermediate state F_{IM} appears to approach infinity when the field direction approaches a hard axis ($\phi \rightarrow 0$, which is equivalent to $\theta \rightarrow 45^\circ$). Below $H \approx 2.7$ T, the following relation is

found to be roughly obeyed: $H_{3f}(\phi) = H_{3f0}/\sin(\phi)$ with $H_{3f0} \approx 0.62$ T.

All critical fields within the range $|\theta| \lesssim 30^\circ$ are found to be proportional to $1/\cos(\theta)$. In this case, field dependences $\tau(H)/H = M(H)\sin(\beta)$ represent $M(H)$ behavior under and between metamagnetic transitions. They show a (upper part of Fig. 1) sharp increases in $M(H)$ at the metamagnetic transitions and more smooth (or nearly field-independent) behavior between them as found previously⁵ for $\text{ErNi}_2\text{B}_2\text{C}$ for $\theta < 30^\circ$.

When the field direction is close to a hard axis, transition to the saturated paramagnetic state proceeds through the intermediate phase F_{IM} (Fig. 4). The transition ($F_{2c} \rightarrow F_{IM}$) at field H_m is accompanied by a dramatic decrease in torque (Figs. 1 and 2) which means that the averaged net magnetization is rotated towards a hard axis. For field direction in the immediate vicinity of a hard axis, the torque is nearly zero after completion of the transition. This implies that the net magnetization is oriented roughly along a hard axis in the phase F_{IM} for $\phi \rightarrow 0$.

If the Er moments align along an easy axis for any metamagnetic state as expected, the phase F_{IM} may be either non-collinear or a mixed state. In either case the net magnetization can be directed along the hard axis with $\phi \rightarrow 0$. Since neutron diffraction studies^{3,4} have revealed no indication of a non-collinear phase, a mixed state appears to be more likely, since easy axes $\langle 100 \rangle$ and $\langle 010 \rangle$ are equivalent for tetragonal symmetry. This is consistent with neutron observation of a two-domain magnetic structure with perpendicular modulation vectors (and, accordingly, ordered moments) equally populated for field direction along a hard axis⁴. Thus, the net magnetization would be directed along this axis as well, providing a basis not only for a satisfactory explanation of zero torque magnitude at $\phi \approx 0$, but also for the origin of the intermediate phase. This phase is probably a two-domain state where domains of each type are saturated paramagnetics with different directions of magnetization. The final transition $F_{IM} \rightarrow F_{PM}$ is thus a transition from the two-domain to a single-domain state. This transition was observed⁵ as a very slight increase in longitudinal magnetization at a critical field that diverged as $\phi \rightarrow 0$, but the nature of the transition was not understood at that time. Results of this torque study make this quite clear.

This research was supported by the Robert A Welch Foundation (A-0514), NSF (DMR-0315476 and DMR-0422949).

* Electronic address: naugle@physics.tamu.edu

† Electronic address: belevtsev@ilt.kharkov.ua

¹ J. Zaretsky et al. Phys. Rev. B **51**, 678 (1995).

² J. W. Lynn et al., Phys. Rev. B **55**, 6584 (1997).

³ A. J. Campbell et al., Sol. State Commun. **115**, 213 (2000).

⁴ A. Jensen et al., Phys. Rev. B **69**, 104527 (2004).

⁵ P. C. Canfield et al., Physica C **262**, 249 (1996).

⁶ P. C. Canfield and S. L. Bud'ko, J. Alloys Compd. **262**, 169 (1997).

⁷ S. L. Bud'ko et al., Phys. Rev. B **61**, R14932 (2000).